Journal of Pathology
J Pathol 2006; **209**: 400–410
Published online 31 March 2006 in Wiley InterScience (www.interscience.wiley.com). **DOI:** 10.1002/path.1980

Original Paper

Endomyocardial infiltration by B and NK cells foreshadows the recurrence of cardiac allograft rejection

C Sorrentino,[1,2†] A Scarinci,[3†] T D'Antuono,[1] M Piccirilli,[4] M Di Nicola,[5] M Pasquale,[3] C Di Iorio[3] and E Di Carlo[1,2*]

[1]*Department of Oncology and Neurosciences, Surgical Pathology Section, 'G. d'Annunzio' University, Chieti, Italy*
[2]*Ce.S.I. Aging Research Centre, 'G. d'Annunzio' University Foundation, Chieti, Italy*
[3]*Medical and Surgical Department of Cardiology, Cardiology Section, 'SS Annunziata' Hospital, Chieti, Italy*
[4]*Department of Applied Sciences of Oral and Dental Diseases, Surgical Pathology Section, 'G. d'Annunzio' University, Chieti, Italy*
[5]*Department of Biomedical Sciences, Laboratory of Biostatistics, 'G. d'Annunzio' University, Chieti, Italy*

**Correspondence to:*
Dr E Di Carlo, Department of Oncology and Neurosciences, Surgical Pathology Section, 'G. d'Annunzio' University, Chieti, Italy.
E-mail: edicarlo@unich.it

[†]*These authors contributed equally to this work.*

Received: 13 September 2005
Revised: 24 January 2006
Accepted: 7 February 2006

Abstract

Heart allograft outcome is unpredictable and acute rejection episodes still occur despite the improvement of immunosuppressive regimens. We therefore investigated whether the immunopathological profile of endomyocardial biopsies might underlie the variations in the clinical course of a graft. Biopsies from transplanted patients were analysed by histology, immunohistochemistry (associated with digital image analysis), confocal and electron microscopy to determine the type and the functional state of leukocytes infiltrating the myocardium, together with their ultrastructural features and those of the graft itself. In comparison with biopsies with grade 0R or grade 1R rejection, those from patients with grade 2R rejection displayed significant infiltration of macrophages, T lymphocytes, and CD83$^+$ and DC-SIGN$^+$ dendritic cells. Fifty-seven per cent were invaded by CD20$^+$B lymphocytes, most of which expressed CD69 activation marker and cooperated in interleukin-12 production, and by CD69$^+$CD94$^+$NK cells expressing interferon-γ. Ultrastructural signs of myocyte degeneration and microvessel rupture by NK cells were frequent. These patients developed recurrent episodes of acute allograft rejection. Endomyocardial B and NK infiltrates are involved in the dynamics of allograft rejection and are associated with a high risk of its recurrence. Immunopathological assessment of endomyocardial biopsies may thus serve to forecast the probable outcome of a heart allograft.

Keywords: immunohistochemistry; electron microscopy; transplantation; leukocytes; cytokines

Introduction

Histopathological study of endomyocardial biopsies (EMBs) in accordance with the criteria established [1] and up-dated [2] in November 2005 by the International Society for Heart and Lung Transplantation (ISHLT), is the main tool for the diagnosis of acute rejection.

Grade (G) 1 (now G 1R) rejection [2] takes the form of a mild, sub-clinical episode marked by a focal or diffuse infiltrate, but no impairment of transplant function, and the immunosuppressive protocol is not modified, whereas G 2 (now included in G 1R), G 3A (now G 2R), and G 3B (now G 3R) rejection are characterized by a more extensive infiltrate with replacement of myocytes and functional impairment. These episodes still occur despite the improvement of immunosuppressive regimens and are the leading cause of allograft loss [3,4].

Acute rejection is the consequence of alloantigen primed T cell infiltration of the graft. Its first step is binding of antigen-presenting cells (APCs) to the host's CD4$^+$T helper (h) cells, followed by cytokine release and cytotoxicity [5]. The mechanisms that elicit such episodes in patients receiving constant immunosuppressive therapy are not known. Immunopathological examination of the transplanted tissue is used to elaborate a cellular and molecular profile for each rejection grade and each patient.

This paper presents a complete immunophenotypical characterization of infiltrating reactive cells in EMBs from patients with no rejection (G 0R) to G 2R, together with the detection of their functional state and release of cytokines. Immunopathological evaluation of EMBs has revealed new morphological parameters with prognostic significance.

Material and methods

Patients and histopathological analyses of endomyocardial biopsies

Twenty-one patients (17 M, 4 F) aged 30–66 who had received a transplant owing to idiopathic dilated cardiomyopathy (15 patients) or ischaemic cardiopathy (6 patients) were enrolled consecutively after transplantation and monitored during the first year after transplantation. All patients were tested for HLA-A, HLA-B, and HLA-DR antigens by serological typing.

Biopsies were performed by trained haemodynamists at the 'SS Annunziata' Hospital, Chieti, Italy, as part of a standard protocol for post-transplant monitoring.

A total of 361 EMBs were obtained during the first year after transplantation: 17 per patient plus 4 required in the light of the clinical assessment. Samples were collected weekly for 4 weeks, fortnightly until 12 weeks, and then monthly. Six biopsies were taken at each sampling time and analysed by two pathologists, EDC and CS. There was almost perfect agreement (κ value $= 0.82$) between their gradings [6].

For histology, four biopsies were fixed in 4% formalin, embedded in paraffin wax, sectioned at 4 μm, and stained with haematoxylin and eosin. For immunohistochemistry and immunofluorescence, one or two biopsies were snap-frozen in liquid nitrogen, and for electron microscopy, one or two biopsies were fixed in cacodylate-buffered 2.5% glutaraldehyde, post-fixed in osmium tetroxide, and embedded in Epon 812. Ultrathin sections were stained with uranyl acetate–lead citrate.

Biopsies were examined according to the original ISHLT criteria [1]. G 0 denotes no infiltrate or very minimal infiltrate. G 1A consists of focal perivascular mononuclear infiltrates. G 1B is characterized by a diffuse interstitial pattern of mononuclear infiltration. G 2 is defined as a single focus of mononuclear infiltration associated with myocyte damage. G 3A shows focal mononuclear infiltrates with replacement of myocytes and functional impairment. G 3B is characterized by diffuse interstitial mononuclear infiltrates, associated with myocyte damage. G 4 consists of widespread damage, conspicuous oedema, and frequent haemorrhage [1]. In 2004, the grading system was revised (R) [2] as follows: grade 0R 'no rejection' (no change from 1990); grade 1R 'mild rejection' (1990 grades 1A, 1B, and 2); grade 2R 'moderate rejection' (1990 grade 3A); and grade 3R 'severe rejection' (1990 grades 3B and 4). The revised grading [2] will be used in the rest of the paper.

Ischaemic injury consists of small focal areas of myocyte damage that may contain mixed inflammatory infiltrates. The Quilty effect is represented by nodular endocardial infiltrates that may be confined to the endocardium (1990 ISHLT Quilty A) or may extend into the myocardium (1990 ISHLT Quilty B) with associated myocyte damage.

All patients received rabbit anti-thymocyte globulin, ciclosporin A, azathioprine, and steroids as reported [7]. In the event of G 2R the protocol is modified [7].

Written informed consent was obtained from patients and the study was approved by the Ethics Committee of the 'SS Annunziata' Hospital. This investigation conformed with the principles outlined in the Declaration of Helsinki.

Immunohistochemistry

For immunohistochemistry on the formalin-fixed, paraffin-embedded samples, sections were incubated for 30 min with the primary antibody (Ab), washed, and incubated with goat anti-mouse immunoglobulin conjugated to peroxidase-labelled dextran (EnVision+™, Peroxidase, mouse) (Dako, Glostrup, Denmark). Immunohistochemistry on the frozen samples was performed as reported previously [8]. Table 1 lists

Table 1. Antibodies used in immunostaining

Antibody	Clone	Origin	Mono/polyclonal	Dilution	Source
Reactive Cells					
CD68	PG-M1	Mouse	Monoclonal	1/30	Dako Glostrup, Denmark
CD83	1H4b	Mouse	Monoclonal	1/5	Novocastra, Newcastle, UK
CD209	DCN46	Mouse	Monoclonal	1/100	Pharmingen, San Diego, CA, USA
CD20	L26	Mouse	Monoclonal	1/100	Dako
CD94	HP-3D9	Mouse	Monoclonal	1/50	Dako
CD4	MT310	Mouse	Monoclonal	1/50	Dako
CD8	C8/144B	Mouse	Monoclonal	1/30	Dako
CD15	C3D-1	Mouse	Monoclonal	1/25	Dako
Endothelial cells					
FVIII	F8/86	Mouse	Monoclonal	1/40	Dako
Activation marker					
CD69	MLR-3	Mouse	Monoclonal	1/50	Dr S Ferrini, Genova, Italy
Cytokines					
IL-12		Rabbit	Polyclonal	1/60	Santa Cruz, Santa Cruz, CA, USA
IFN-γ		Goat	Polyclonal	1/40	Santa Cruz
IL-10	E-10	Mouse	Monoclonal	1/5	Santa Cruz

the Abs and dilutions. Biotinylated horse anti-mouse or anti-goat Ab or biotinylated goat anti-rabbit Ab (all from Vector Laboratories, Burlingame, CA, USA) were used as secondary Abs.

Viral infections were tested on paraffin-embedded tissue sections as published [9–11]. Automated cell counts [12] and analyses of cytokine expression [8] were performed by light microscopy on single immunostained sections with Qwin image analysis software (version 2.7), which has the following highly reproducible steps: (1) image acquisition; (2) conversion of RGB image (true colour) to binary image (black and white); (3) filtering to remove noise; (4) counting of immunostained cells or measurement of positively stained area.

In EMBs with G 1R, G 2R, ischaemic injury, and Quilty lesions, reactive cells were only counted in fields containing the inflammatory foci, whereas in G 0R biopsies, fields were randomly chosen.

For each reactive cell marker or cytokine, three high-power fields were analysed for each section and three sections per biopsy were evaluated.

Single and double immunofluorescence and confocal microscopy

To test biopsies for complement components, the indirect immunofluorescence method was performed on acetone-fixed frozen sections as reported [13]. For co-localization studies, double immunofluorescent staining was performed on acetone-fixed frozen sections as reported [8] and analysed under a Zeiss LSM 510 Meta confocal microscope (Zeiss, Oberkochen, Germany).

Statistical analysis

Variables are reported as mean and standard deviation (SD). The hypotheses of normality of the distribution of the reactive cells were assessed with the Kolmogorov–Smirnov test. Differences between the rejection grade for each reactive cell were evaluated with a one-way analysis of variance (ANOVA) test. The difference between each pair of means was evaluated using the Tukey pairwise multiple comparisons test. All statistical tests were evaluated at an α level of 0.05. Statistical analysis was carried out with SPSS software, version 11.0 (SPSS Inc, Chicago, IL, USA).

Results

Histological and immunohistochemical features of EMBs

The 361 EMBs obtained from 21 patients during the first year after transplantation were grouped by rejection grade as follows: G 0R, 159; G 1R, 175 (1990 grades: 92 G 1A, 76 G 1B, and 7 G2. EMBs with G2 were discarded because serial sections revealed an underlying G 3A or a 'Quilty effect' [14]); G 2R, 25; G 3R, 2 (1990: 2 EMBs with G 3B and no EMB with G 4).

G 1R is also described as 'mild' rejection and compared with G 2R or 'moderate' rejection and G 0R or 'no' rejection. Furthermore, 134 EMBs showed a Quilty effect (1990: 71 Quilty B plus 63 Quilty A) and 13 showed ischaemic injury.

Figure 1 illustrates features of G 0R, G 1R, and G 2R.

Table 2 shows the mean content of the reactive cells evaluated from 25 G 0R, 50 G 1R (1990: 25 G 1A plus 25 G 1B. Data from G 1R EMBs were homogeneous, ie no substantial differences emerged in the number of infiltrating reactive cells nor in cytokine expression between G 1A and G 1B EMBs) and 25 G 2R (the number of biopsies analysed for each rejection grade was dictated by the available number of G 2R biopsies). EMBs with G 2R were obtained from 14/21 patients. EMBs with G 0R and those with G 1R were randomly chosen from all 21 patients after the exclusion of inadequate biopsy sets and biopsies positive for viral infections.

Inflammatory cells infiltrating the graft

The EMB reactive cell content increased and changed in quality as a function of the rejection grade (Table 2).

DC-SIGN$^+$ (CD209) cells were evenly distributed among the cardiomyocytes in the G 0R EMBs, whereas they accumulated perivascularly in G 1R and G 2R and were also increased in the latter (Figures 2a,

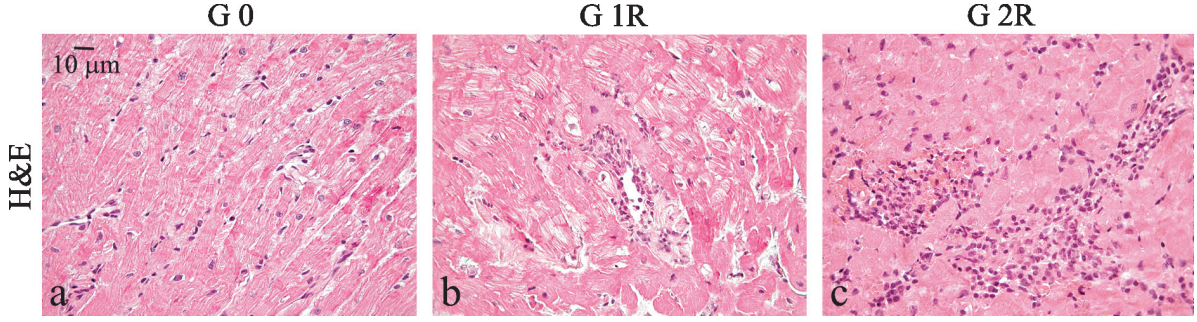

Figure 1. Histological features of EMBs with G 0R, G 1R, or G 2R rejection. According to the ISHLT, a biopsy with scattered, very occasional mononuclear cells is classed as G 0R, that with one focus of perivascular mononuclear cells is classed as G 1R, and that with two or more foci of reactive cells is classed as G 2R rejection.(a–c: ×400)

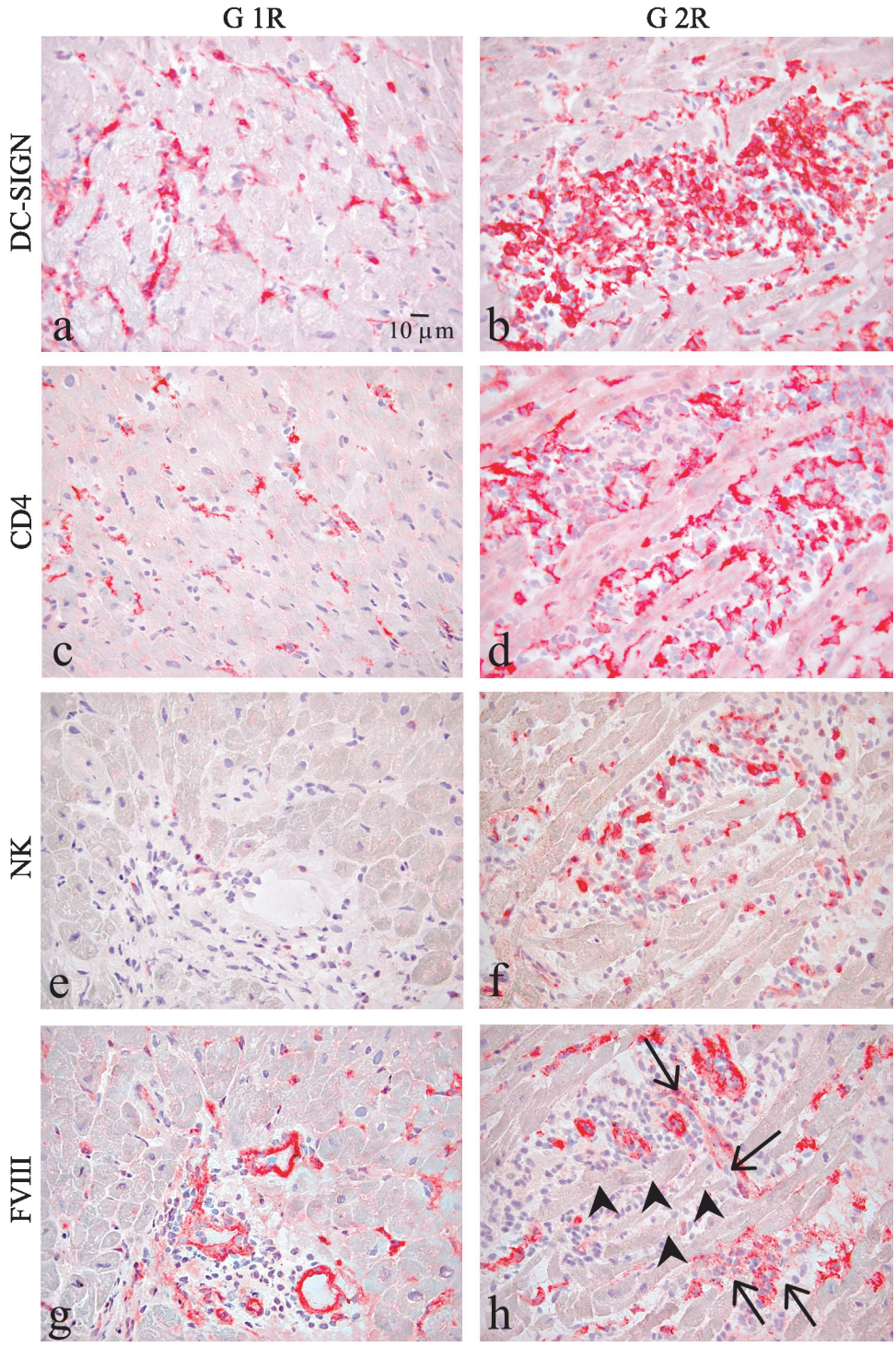

Figure 2. Reactive cell recruitment in G 1R and G 2R EMB. A substantial recruitment of DC-SIGN$^+$DCs (b) and CD4$^+$T lymphocytes (d) is observed in G 2R (group A) in comparison with G 1R biopsies (a and c, respectively). In EMB with G 1R rejection, NK cells are absent (e) and microvessels intact (g). In a G 2R EMB, particularly in sub-type A, signs of myocyte (arrowheads) and endothelial cell (arrows) damage (h) are evident in association with significant NK cell recruitment (f). (a–h: ×400)

b). They were the only leukocyte population well represented in the G 0R EMBs, where macrophages (CD68) and lymphocytes were barely detected. Expression of the dendritic cell (DC) maturation marker, CD83, almost undetectable in the G 0R EMBs, was very weak in G 1R and increased in G 2R.

CD4$^+$T cells significantly ($p < 0.05$) increased from G 0R to G 1R. They formed the majority of all graft infiltrating cells in G 2R (Figures 2c, d). The CD4$^+$/CD8$^+$T cell ratio increased from 1.6 in G 1R to 2.4 in G 2R, since the CD4$^+$T lymphocyte increase was greater than the CD8$^+$T lymphocyte increase. Macrophages and CD4$^+$T cells increased about four and three times respectively, while CD8$^+$T cells doubled from G 1R to G 2R. However, the increase (about eight times) in the number of CD20$^+$B and NK cells

Table 2. Mean content of the reactive cell populations in groups of EMBs with G 0R, G 1R or G 2R rejection

Reactive cells*	Rejection grade G 0R ($n = 25$)	G 1R ($n = 50$)	G 2R ($n = 25$)	ANOVA† p value
CD68	3.0 ± 1.0	$5.0 \pm 1.0^{\ddagger}$	$15.0 \pm 3.0^{\ddagger\S}$	<0.001
CD83	1.0 ± 0.2	$2.0 \pm 0.5^{\ddagger}$	$9.0 \pm 2.0^{\ddagger\S}$	<0.001
CD209	12.0 ± 2.0	$10.0 \pm 2.0^{\ddagger}$	$18.0 \pm 3.0^{\ddagger\S}$	<0.001
CD20	0.7 ± 0.5	1.0 ± 0.3	$10.0 \pm 2.0^{\ddagger\S}$	<0.001
CD94	0.2 ± 0.3	$1.0 \pm 0.4^{\ddagger}$	$9.0 \pm 2.0^{\ddagger\S}$	<0.001
CD4	1.0 ± 0.1	$8.0 \pm 2.0^{\ddagger}$	$24.0 \pm 4.0^{\ddagger\S}$	<0.001
CD8	3.0 ± 1.0	$5.0 \pm 1.0^{\ddagger}$	$10.0 \pm 2.0^{\ddagger\S}$	<0.001
CD15	0.0 ± 0.0	2.0 ± 0.8	$4.0 \pm 1.0^{\ddagger\S}$	<0.001

* Reactive cells were counted by light microscopy, at ×400 in an 85431.59 μm^2 field, on single immunostained formalin-fixed, paraffin-embedded (CD68, CD83, CD20, CD8, CD15) or cryostat sections (CD209, CD94, CD4). Results are mean ± SD of positive cells/field.
† One-way ANOVA for comparisons between three rejection grades and for each reactive cell.
‡ $p < 0.05$ Tukey test compared with G 0R;
§ with G 1R.

(CD94) (Figures 2e, f), which were usually absent or very rare in both G 0R and G 1R rejection, was more substantial. In association with perivascular foci of high NK cell recruitment, EMBs with G 2R frequently displayed signs of microvessel wall injuries, as shown by FVIII staining (Figures 2g, h).

Granulocytes (CD15) were absent in G 0R EMBs and barely detectable in G 1R and G 2R EMBs (Table 2).

Inflammatory cells in ischaemic injury and Quilty lesions

Since ischaemic injury and Quilty lesions, particularly the B sub-type, are potential histological mimics of acute cellular rejection [15,16], we also analysed these lesions and made a comparison with G 2R (Figure 3).

Ischaemic injury was observed in 13 very early (within the first 2 weeks) post-transplant EMBs. Immunophenotyping revealed a prevailing macrophage ($CD68 = 46 \pm 9$) infiltrate and numerous granulocytes ($CD15 = 27 \pm 6$), which were significantly ($p < 0.05$) more represented than in G 2R. $CD4^+$ and $CD8^+$T lymphocytes were also present (respectively, 15 ± 4 and 9 ± 3), whereas NK cells were barely detected ($CD94 = 4 \pm 1$) and $CD20^+$B lymphocytes were
absent.

Quilty B lesions (25 randomly chosen biopsies) showed a prevalent infiltration of $CD4^+$T lymphocytes and $CD20^+$B lymphocytes ($CD4 = 92 \pm 16$; $CD20 = 68 \pm 11$). $CD8^+$T lymphocytes were also numerous ($CD8 = 57 \pm 12$) as were macrophages ($CD68 = 35 \pm 8$), while NK cells and granulocytes were barely detected ($CD94 = 5 \pm 2$; $CD15 = 6 \pm 3$). T and B lymphocytes and macrophages were more represented in Quilty B lesions than in G 2R.

Immunophenotyping of G 2R EMBs

We excluded the most common viral infections as a co-factor of the inflammatory reaction observed in G 2R EMBs, since they were negative for enterovirus, cytomegalovirus, and Epstein–Barr virus infections. Humoral rejection [17] was also ruled out as a cause of B cell infiltrate in G 2R EMBs, since they were negative for C4d and C3d.

Next, we placed the EMBs from the eight patients who developed more than one episode of G 2R in group A, and those from the six patients who developed only one episode in group B. The degrees of HLA mismatching in G 2R groups A and B ranged from 4 to 6. Five group A patients developed two G 2R episodes; the other three developed three (two consecutively in one patient). With the exception of this patient, episodes were separately by from 1 to 3 EMBs graded G 0R or G 1R. Table 3 reports the time points at which each biopsy with G 2R rejection was drawn.

Immunophenotyping of these biopsies showed, contrary to G 0R and G 1R rejection, the presence of

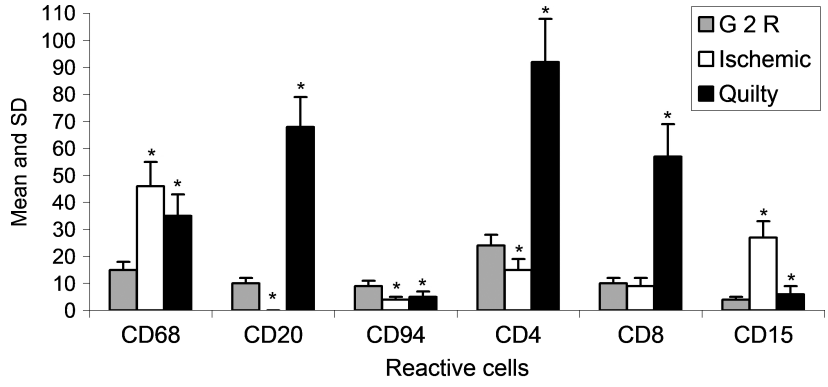

Figure 3. Mean content of the reactive cells in groups of EMBs with ischaemic injury and Quilty lesions versus group of EMBs with G 2R. Grey bars represent the mean ± SD of a reactive cell population in G 2R EMBs (n = 25). White bars represent the mean ± SD of a reactive cell population in EMBs with ischaemic injury (n = 13). Black bars represent the mean ± SD of a reactive cell population in EMBs with Quilty lesions (n = 25)

Table 3. Distribution of G 2R biopsy times during the first year after transplantation

		Time after transplantation (months)																
		1				2		3		4	5	6	7	8	9	10	11	12
Patients	Number of G2R EMBs	1st	2nd	3rd	4th	5th	6th	7th	8th	9th	10th	11th	12th	13th	14th	15th	16th	17th
1	3					×				×	×							
2	3								×				×		×			
3	3										×			×		×		
4	2							×				×						
5	2													×			×	
6	2								×			×						
7	2								×				×					
8	2				×			×										
1	1						×											
2	1										×							
3	1									×								
4	1													×				
5	1								×									
6	1												×					

Table 4. Mean content of the reactive cell populations and expression of immunoregulatory molecules in EMBs from the two groups (A and B)* of patients with G 2R rejection

Rejection group*	Reactive cells†							Cytokines‡		
	CD68	CD83	CD209	CD20	CD94	CD4	CD8	IL-12	IFN-γ	IL-10
A	15 ± 2	11 ± 2	20 ± 5	14 ± 3	17 ± 3	28 ± 4	14 ± 2	11.8 ± 2.2	5.7 ± 1.2	10.1 ± 1.5
B	12 ± 1	6 ± 2	15 ± 2	4 ± 1§	5 ± 2§	21 ± 3	8 ± 3	3.2 ± 1.0§	1.5 ± 1.3§	9.8 ± 1.7

* Group A: eight patients who developed more than one G 2R rejection episode (a total of 19 biopsies). Group B: six patients who developed only one episode of G 2R rejection (a total of six biopsies), as reported in 'Material and Methods'.
† Cell counts were performed by light microscopy, at ×400 in an 85431.59 μm^2 field, on single immunostained formalin-fixed, paraffin-embedded (CD68, CD83, CD20, CD8) or cryostat sections (CD209, CD94, CD4). Results are mean ± SD of positive cells/field.
‡ Cytokine expression values were represented as the mean percentage of positively stained areas/total area of the examined field (85431.59 μm^2).
§ $p < 0.05$, Mann–Whitney U test from values in EMBs of group A.

endomyocardial $CD20^+$B cell and $CD94^+$NK cell infiltrates usually organized in perivascular sheets. Interestingly, the mean content of $CD20^+$B lymphocytes and $CD94^+$NK cells in EMBs from the group A patients was significantly ($p < 0.05$) higher than that in group B (Figure 4 panel A, a, b; Table 4).

Furthermore, the double immunofluorescence staining of EMBs with G 2R (group A) showed that most endomyocardial infiltrating $CD20^+$B cells expressed the CD69 activation marker (Figure 4 panel A, c). CD69 was also frequently detected on $CD94^+$NK and T cells (data not shown).

Quantification of other leukocyte sub-populations disclosed a trend towards an increase in the mean content of DC, $CD4^+$ and $CD8^+$T lymphocytes in the group A EMBs, though the difference between the two groups was not statistically significant (Table 4).

No significant association was found, by using Mann–Whitney U test or the χ^2 test, between groups A and B and variables such as host and donor age, host weight, diagnosis before transplantation, and HLA mismatches.

Notably, no significant differences emerged in the number of leukocytes or in cytokine expression between G 1R episodes that preceded, or did not precede, G 2R episodes.

Table 4 shows the mean content of the reactive cell populations and the cytokine expression in groups A and B.

Expression of Th1 and Th2 cytokines by graft infiltrating cells

We investigated intragraft expression of the Th1 cytokines interleukin (IL)-12 and interferon-γ (IFN-γ), and the Th2 cytokine IL-10, since the former play a key role in experimental transplant rejection models [18,19], while the latter displays immunosuppressive and regulatory functions [20,21] and prolongs allograft survival [22].

Production of IL-12 was absent in G 0R EMB (0.3 ± 0.1) and scanty in G 1R (1.8 ± 0.7). IL-12 was strongly expressed in G 2R EMBs (Figure 4 panel B, a–c) from group A (11.8 ± 2.2) and scanty to moderate (3.2 ± 1.0) in those from group B ($p < 0.05$). Cooperation of macrophages in IL-12 production by graft infiltrating cells has been reported [23]. Our confocal analyses showed that IL-12 co-located with DC-$SIGN^+$ DC and more frequently with $CD20^+$B cells (Figure 5).

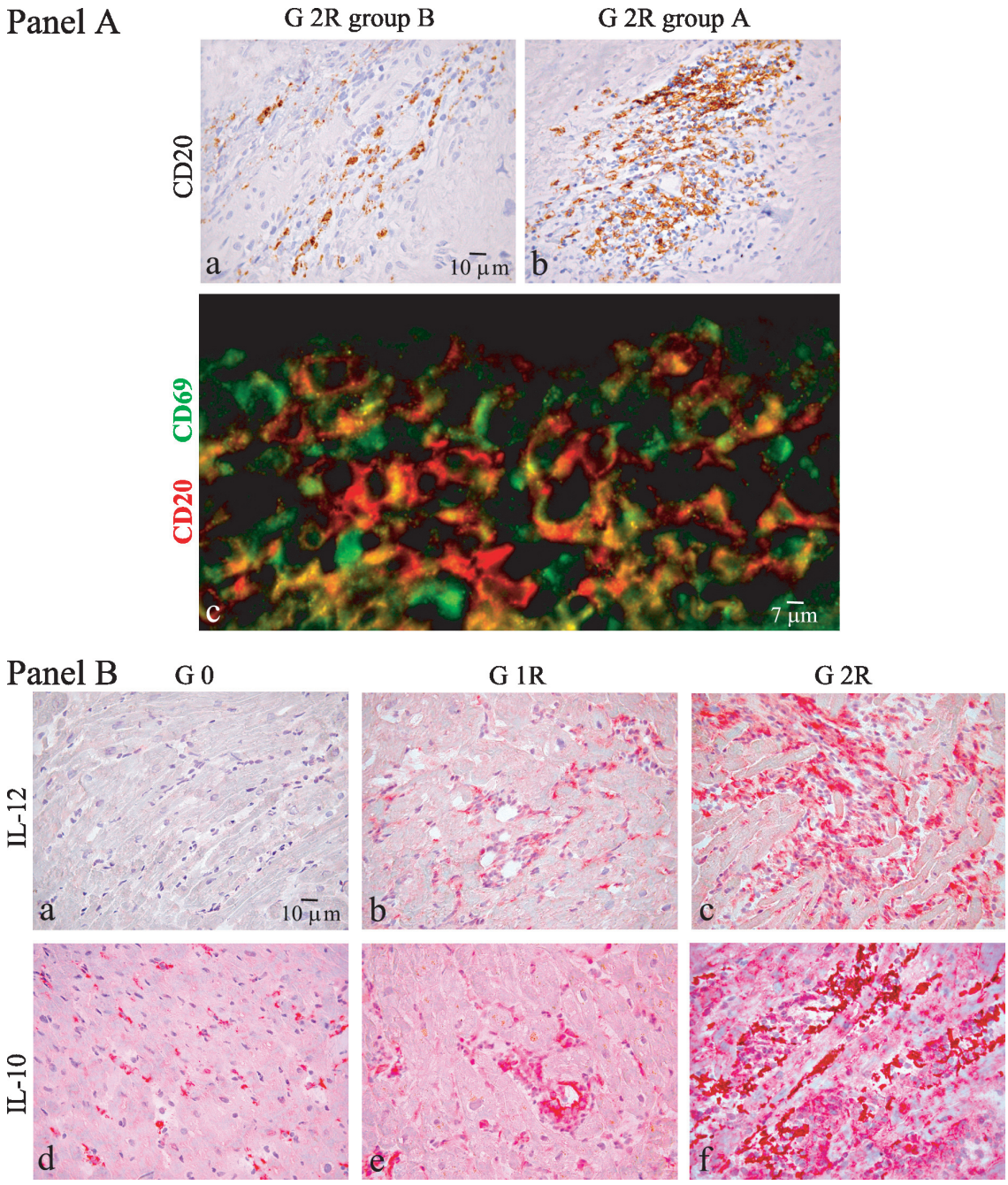

Figure 4. Panel A. Infiltration by activated B lymphocytes in EMBs with G 2R rejection. The content of $CD20^{+}$B lymphocytes in group A EMBs (b) was significantly higher than that in group B (a). Most B lymphocytes (c, red) expressed CD69 activation marker (c, green) as shown by their partial co-localization indicated by the yellow-colour. (a–c: ×400). Panel B. Expression of interleukin (IL)-12 and IL-10 in G 0R, G 1R, and G 2R EMBs. IL-12 was absent in EMBs classed as G 0R (a) and barely detectable in those with G 1R rejection (b), while it was strongly expressed in G 2R EMBs (c). Strong production of IL-10 was usually found in G 2R EMBs (f), while it was weaker, but clearly detectable, in most G 1R EMBs (e) and scanty, but also clearly expressed in most G 0R EMBs (d). (a–f: ×400)

IFN-γ was undetectable in all the G 0R (0.1 ± 0.1) and half of the G 1R EMB (0.6 ± 0.3), and scanty in the rest (2.0 ± 0.8). It was almost absent in group B EMBs (1.5 ± 1.3) and moderate in group A (5.7 ± 1.2) ($p < 0.05$) (Table 4). IFN-γ staining was usual in close proximity to T cell tissue distribution and, in G 2R EMBs, frequently co-located with NK cells (data not shown).

IL-10 was scanty, but also clearly expressed in most G 0R EMB (2.6 ± 0.4). Its strong production was usual in most G 2R EMBs (group A: 10.1 ± 1.5; group B: 9.8 ± 1.7) (Figure 4 panel B, d–f; Table 4) while it was weaker, but clearly detectable (6.3 ± 1.5), in most G 1R EMB.

Ultrastructural features of G 2R EMB

Group A EMBs frequently showed severe myocardial degeneration characterized by extensive intracytoplasmic vacuolation, frequent myelin figures, abnormal

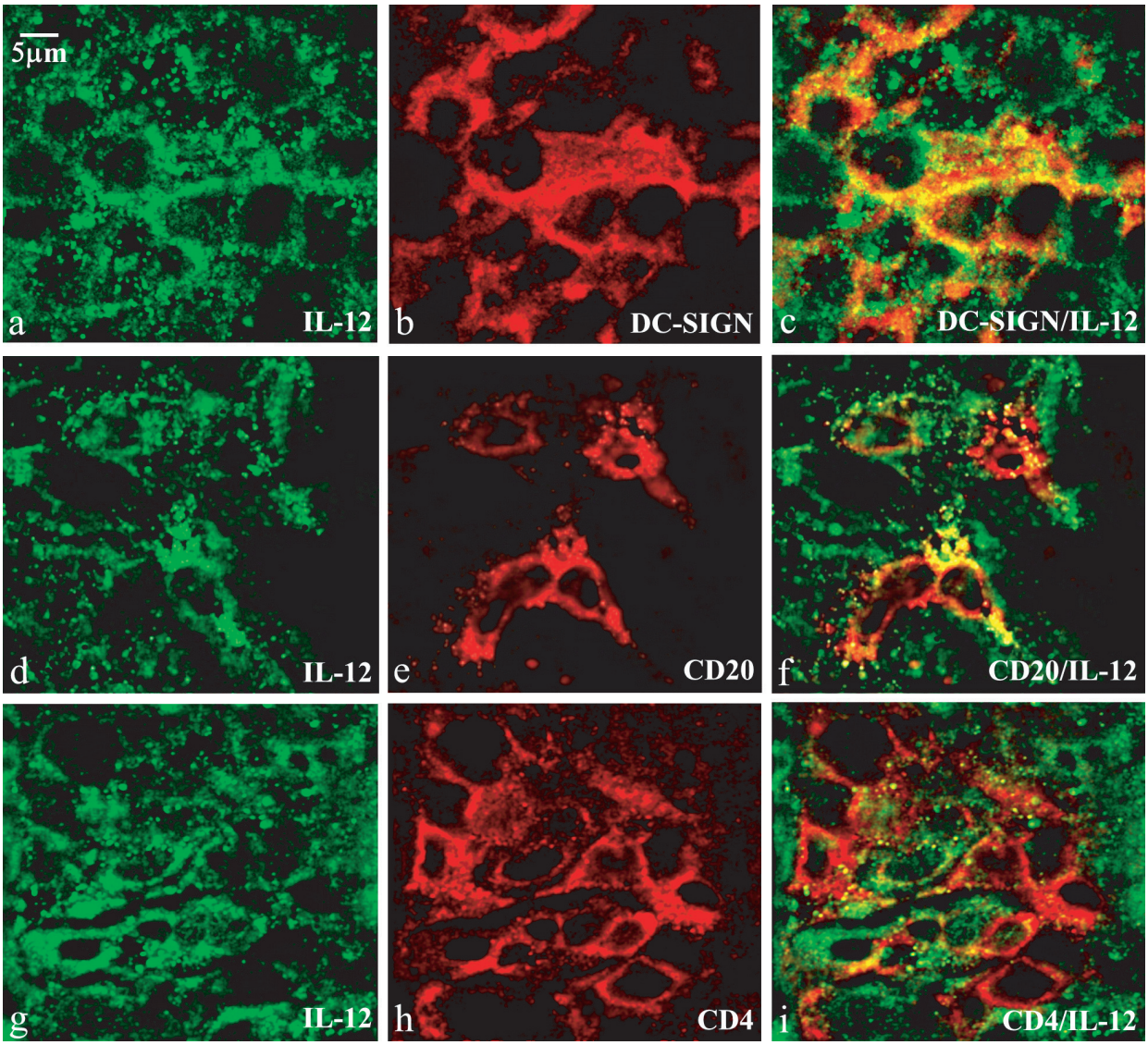

Figure 5. Confocal images of IL-12 production in a G 2R EMB. The expression of IL-12 (a, d, g: green) co-localizes with DC-SIGN$^+$ DCs (b: red), and partially with CD20$^+$B lymphocytes (e: red) as shown by the merged images c and f, respectively (yellow), and is found close (i) to some CD4$^+$T cells (h: red) ($\times$1000)

Z bands, increased nuclear convolution, and irregular mitochondria (Figure 6a), whereas the group B EMBs usually displayed moderate myocardial degeneration, characterized by the appearance of myelin figures and less extensive mitochondrial alterations, myofibrillar disarray, and myocyte vacuolation (Figure 6b).

Group A EMBs revealed more frequent infiltration of cells with the features of NK cells (Figures 6c, d arrows) endowed with evident mitochondria, dense granules, and empty vesicles (Figure 6e) resulting from exocytosis. These cells were frequently found among widespread erythrocytes coming out from injured microvessels (Figures 6d, e).

Discussion

Our investigations show that (1) CD4$^+$T lymphocytes are the main participants in the inflammatory reaction governing the lower grade of heart allograft rejection, since their number significantly increased from G 0R to G 1R; (2) the transition to G 2R (myocyte replacement or damage by infiltrating cells) is marked by a prevalent infiltration of APCs, namely macrophages, mature and immature DCs, which may release IL-12, associated with significant recruitment of T lymphocytes, some of which express IFN-γ. Surprisingly, G 2R rejection may be accompanied by a substantial infiltration of activated B and NK cells which cooperate in IL-12 and IFN-γ expression and allow identification of a sub-group of G 2R patients (57% of our cohort) with a high risk of rejection recurrence and development of immunosuppressive drug resistance. This finding indicates that immunophenotyping of EMBs with G 2R may predict the individual response to post-transplant treatment, and suggest cellular and molecular targets to prevent allograft failures.

In addition, since most G 2R episodes occur in the 'early' post-transplant period, ie the first 6 months [our data and refs 24,25], immunophenotypic analyses

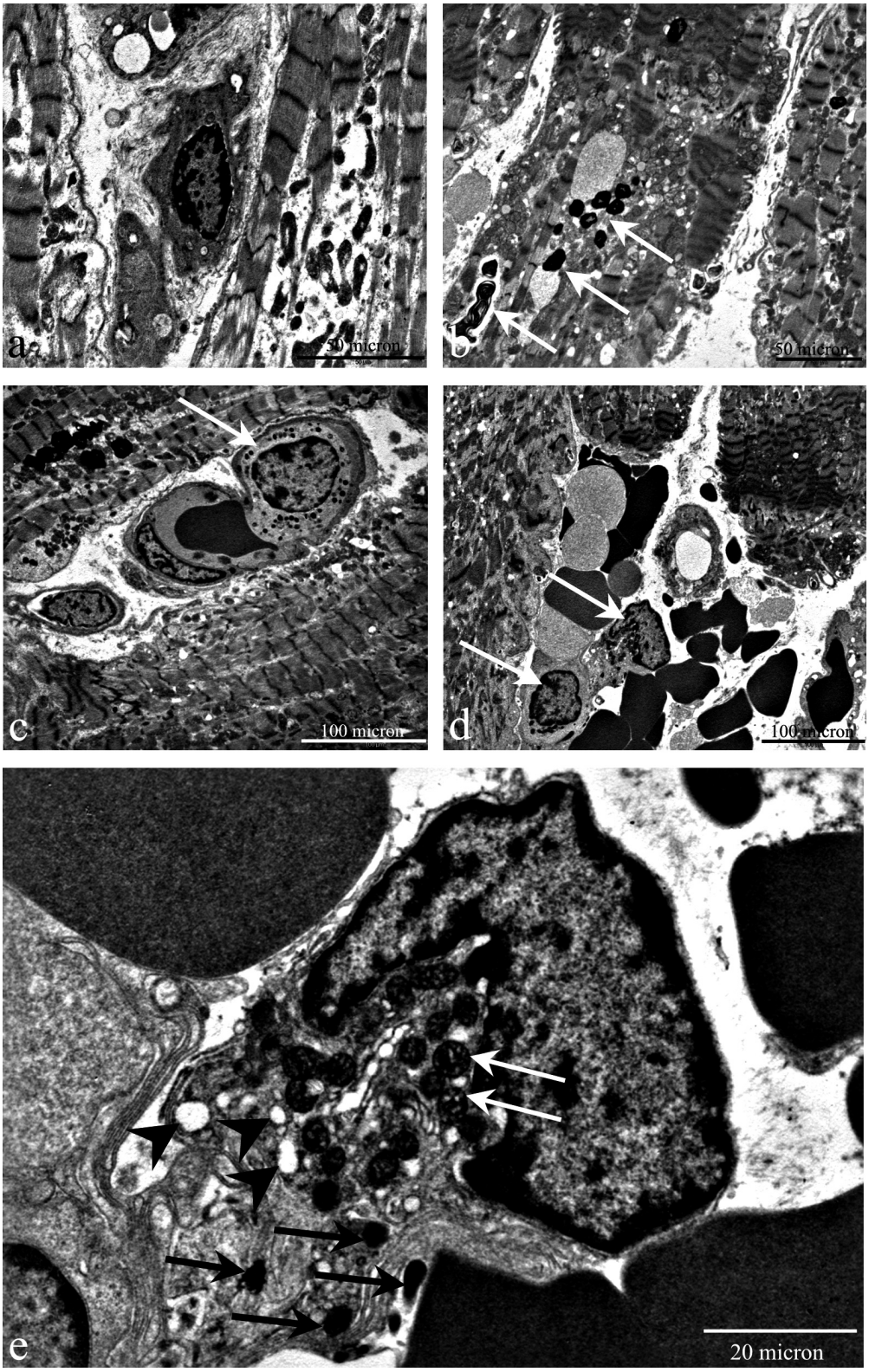

Figure 6. Ultrastructural features of the two sub-types of G 2R EMB. (a) Electron micrograph of group A G 2R EMB showing severe myocardial degeneration characterized by extensive intracytoplasmic vacuolation, abnormal Z bands, increased nuclear convolution, and irregular mitochondria, whereas (b) group B EMBs usually displayed moderate myocardial degeneration with the appearance of myelin figures (arrows) and less extensive mitochondrial alterations, myofibrillar disarray, and myocyte vacuolation compared with group A. (c) EMB with G 2R rejection showing an intact microvessel filled by a mononuclear cell with the features of an NK cell containing numerous cytoplasmic dense granules (arrow). (d) Two NK cells (arrows), endowed with a cytoplasm containing evident mitochondria, dense granules, but also empty vesicles resulting from exocytosis, are found among widespread erythrocytes, suggesting recent breakdown of endothelial walls. (e) Magnification of a detail of the previous image shows that the pocket between two cells contains membrane vesicles, a feature typical of large granular lymphocyte exocytosis (cytoplasmic granules indicated by black arrows, empty vesicles by black arrowheads, and mitochondria indicated by white arrows)

should have greater prognostic value when performed in this latency time.

After excluding viral infections and humoral rejection as possible causes of B lymphocyte infiltrates, the immunopathological profile of G 2R is easily distinguishable from that of ischaemic injury and Quilty lesions [15,16]. The first, in fact, is marked by the absence of B lymphocytes and the presence of a marked macrophage and neutrophil infiltrate, the second by very florid $CD20^+$B cell and $CD4^+$T cell recruitment which was much more substantial than in G 2R biopsies.

Immunophenotyping of EMBs revealed that DCs bearing DC-SIGN, expressed on immature and maturing DCs [26] and central to their trafficking capacity [27], increased in G 2R. We speculate that DC-$SIGN^+$ cells have a dual role in transplantation. As immature DCs, they suppress peripheral T cell responses to foreign antigens, and induce transplant tolerance [28] in G 0R. On the other hand, in G 1R, and particularly in the group A of G 2R EMB, the perivascular accumulation of IL-12-producing DC-$SIGN^+$ cells in the inflammatory foci [29], tightly intermingled with the recruited T cells, enables transient DC–T cell interaction and facilitates primary immune responses [27].

It has been reported that immunosuppressive drugs (eg corticosteroids) inhibit DC maturation and inflammatory cytokine production [30]. We partially confirm this finding in patients who had received a transplant, since DCs bearing the CD83 maturation marker were almost absent in G 1R and occasionally increased in G 2R EMBs. However, IL-12 was clearly detected in DC-$SIGN^+$ DCs, suggesting that an escape mechanism from pharmacological suppression has developed that results in local inflammatory response activation. These EMBs also showed significant macrophage infiltration and perivascular recruitment of $CD20^+$B cells, which resist pharmacological suppression better than macrophages [31,32]. A striking association between dense $CD20^+$B cell infiltrate and clinical glucocorticoid resistance and graft loss has been recently described in renal allografts [33]. In the case of cardiac rejection, our finding of IL-12 co-localization with activated B cells strongly supports their role as APCs for indirect allorecognition [34].

In G 2R, IL-12 released by APCs polarizes the immune response towards a Th1 type with induction of INF-γ [18]. The IL-12-dependent Th1 pathway does not seem, however, solely to govern rejection, since it coexists in a complex balance with IL-10 whose expression is favoured by corticosteroids [35]. IL-10 was found in both 'mild' and 'no' rejection EMBs and was more expressed in 'moderate' rejection EMBs, with no differences between groups A and B. In previous studies, IL-10 mRNA and protein expression in EMBs was proportional to the degree of rejection [23,36]. IL-10-releasing Th2 cells are associated with tolerance and may regulate indirect Th1 alloimmune responses in G 0R or G 1R. However, the pro-inflammatory functions of high level IL-10 [37,38], such as that found in G 2R EMBs, and its involvement in the development of corticosteroid resistance cannot be ruled out.

NK cells were slightly and substantially increased in mild and moderate rejection, respectively, in comparison with G 0R. Particularly in group A of G 2R EMBs, activated NK cells accumulated in perivascular sheets and cooperated with T lymphocytes in IFN-γ production. NK cells with exocytic vesicles were frequently found close to injured endothelial walls. NK-cell-mediated [39] microvessel injury may impair myocyte architecture and function, and constitute an important event in allograft behaviour [40]. Like B cells and contrary to alloreactive T cells, NK cells are resistant to ciclosporin, a condition that points to their involvement in the development of immunosuppressive drug resistance [41].

Our results strongly suggest that DC-$SIGN^+$ DCs and B cells other than macrophages, and NK cells other than T cells, are key promoters and effectors, respectively, in allograft rejection.

In addition, B and NK cells are indicative of a high risk of rejection recurrence and appear to be involved in the pathogenesis of immunosuppressive drug resistance. Immunophenotyping of EMBs may be predictive of graft outcome and useful for tailoring the treatment of patients who have received a transplant.

Acknowledgements

This work is supported by a grant awarded by Fondazione Cassa di Risparmio della Provincia di Chieti (CariChieti), Italy. We thank Professor John Iliffe for editing the manuscript.

References

1. Billingham ME, Cary NR, Hammond ME, Kemnitz J, Marboe C, McCallister HA, *et al*. A working formulation for the standardization of nomenclature in the diagnosis of heart and lung rejection: Heart Rejection Study Group. The International Society for Heart Transplantation. *J Heart Transplant* 1990;**9:**587–593.
2. Stewart S, Winters GL, Fishbein MC, Tazelaar HD, Kobashigawa J, Abrams J, *et al*. Revision of the 1990 working formulation for the standardization of nomenclature in the diagnosis of heart rejection. *J Heart Lung Transplant* 2005;**24:**1710–1720.
3. Gallo P, Agozzino L, Angelini A, Arbustini E, Bartoloni G, Bernucci P, *et al*. Causes of late failure after heart transplantation: a ten-year survey. *J Heart Lung Transplant* 1997;**16:**1113–1121.
4. Taylor DO, Edwards LB, Boucek MM, Trulock EP, Deng MC, Keck BM, *et al*. Registry of the International Society for Heart and Lung Transplantation: twenty-second official adult heart transplant report–2005. *J Heart Lung Transplant* 2005;**24:**945–955.
5. Wong BW, Rahmani M, Rezai N, McManus BM. Progress in heart transplantation. *Cardiovasc Pathol* 2005;**14:**176–180.
6. Landis JR, Koch GG. The measurement of observer agreement for categorical data. *Biometrics* 1977;**33:**159–174.
7. McGoon MD, Fronty RP. Techniques of immunosuppression after cardiac transplantation. *Mayo Clin Proc* 1992;**67:**586–595.
8. Di Carlo E, Cappello P, Sorrentino C, D'Antuono T, Pellicciotta A, Giovarelli M, *et al*. Immunological mechanisms elicited at the tumour site by lymphocyte activation gene-3 (LAG-3) versus IL-12: sharing a common Th1 anti-tumour immune pathway. *J Pathol* 2005;**205:**82–91.
9. Zhang H, Li Y, Peng T, Aasa M, Zhang L, Yang Y, *et al*. Localization of enteroviral antigen in myocardium and other

tissues from patients with heart muscle disease by an improved immunohistochemical technique. *J Histochem Cytochem* 2000;**48:**579–584.
10. Plachter B, Nordin M, Wirgart BZ, Mach M, Stein H, Grillner L, *et al*. The DNA-binding protein P52 of human cytomegalovirus reacts with monoclonal antibody CCH2 and associates with the nuclear membrane at late times after infection. *Virus Res* 1992;**24:**265–276.
11. Ganne V, Siddiqi N, Kamaplath B, Chang CC, Cohen EP, Bresnahan BA, *et al*. Humanized anti-CD20 monoclonal antibody (Rituximab) treatment for post-transplant lymphoproliferative disorder. *Clin Transplant* 2003;**17:**417–422.
12. Jacobs JJ, Lehe C, Cammans KD, Yoneda K, Das PK, Elliott GR. An automated method for the quantification of immunostained human Langerhans cells. *J Immunol Methods* 2001;**247:**73–82.
13. Rodriguez ER, Skojec DV, Tan CD, Zachary AA, Kasper EK, Conte JV, *et al*. Antibody-mediated rejection in human cardiac allografts: evaluation of immunoglobulins and complement activation products C4d and C3d as markers. *Am J Transplant* 2005;**5:**2778–2785.
14. Stewart SC, Cary NRB, Goddard MJ, Billingham ME. *Atlas of Biopsy Pathology for Heart and Lung Transplantation*. Arnold: London, 2000; 18.
15. Michaels PJ, Kobashigawa J, Laks H, Azarbal A, Espejo ML, Chen L, *et al*. Differential expression of RANTES chemokine, TGF-beta, and leukocyte phenotype in acute cellular rejection and quilty B lesions. *J Heart Lung Transplant* 2001;**20:**407–416.
16. Marboe CC, Billingham M, Eisen H, Deng MC, Baron H, Mehra M, *et al*. Nodular endocardial infiltrates (Quilty lesions) cause significant variability in diagnosis of ISHLT Grade 2 and 3A rejection in cardiac allograft recipients. *J Heart Lung Transplant* 2005;**24**(Suppl):S219–S226.
17. Colvin RB, Smith RN. Antibody-mediated organ-allograft rejection. *Nat Rev Immunol* 2005;**5:**807–817.
18. Gately MK, Renzetti LM, Magram J, Stern AS, Adorini L, Gubler U, *et al*. The interleukin-12/interleukin-12-receptor system: role in normal and pathologic immune responses. *Annu Rev Immunol* 1998;**16:**495–521.
19. Filatenkov AA, Jacovetty EL, Fischer UB, Curtsinger JM, Mescher MF, Ingulli E. CD4 T cell-dependent conditioning of dendritic cells to produce IL-12 results in CD8-mediated graft rejection and avoidance of tolerance. *J Immunol* 2005;**174:**6909–6917.
20. Tiao MM, Lu L, Tao R, Wang L, Fung JJ, Qian S. Prolongation of cardiac allograft survival by systemic administration of immature recipient dendritic cells deficient in NF-kappaB activity. *Ann Surg* 2005;**241:**497–505.
21. Hara M, Kingsley CI, Niimi M, Read S, Turvey SE, Bushell AR, *et al*. IL-10 is required for regulatory T cells to mediate tolerance to alloantigens in vivo. *J Immunol* 2001;**166:**3789–3796.
22. David A, Chetritt J, Guillot C, Tesson L, Heslan JM, Cuturi MC, *et al*. Interleukin-10 produced by recombinant adenovirus prolongs survival of cardiac allografts in rats. *Gene Ther* 2000;**7:**505–510.
23. Van Hoffen E, Van Wichen D, Stuij I, De Jonge N, Klopping C, Lahpor J, *et al*. In situ expression of cytokines in human heart allografts. *Am J Pathol* 1996;**149:**1991–2003.
24. van Besouw NM, Zuijderwijk JM, Vaessen LM, Balk AH, Maat AP, van der Meide PH, *et al*. The direct and indirect allogeneic presentation pathway during acute rejection after human cardiac transplantation. *Clin Exp Immunol* 2005;**141:**534–540.
25. Meiser BM, Groetzner J, Kaczmarek I, Landwehr P, Muller M, Jung S, *et al*. Tacrolimus or cyclosporine: which is the better partner for mycophenolate mofetil in heart transplant recipients? *Transplantation* 2004;**78:**591–598.
26. Geijtenbeek TB, Engering A, Van Kooyk Y. DC-SIGN, a C-type lectin on dendritic cells that unveils many aspects of dendritic cell biology. *J Leukocyte Biol* 2002;**71:**921–931.
27. van Kooyk Y, Geijtenbeek TB. A novel adhesion pathway that regulates dendritic cell trafficking and T cell interactions. *Immunol Rev* 2002;**186:**47–56.
28. Jonuleit H, Schmitt E, Schuler G, Knop J, Enk AH. Induction of interleukin 10-producing, nonproliferating CD4(+) T cells with regulatory properties by repetitive stimulation with allogeneic immature human dendritic cells. *J Exp Med* 2000;**192:**1213–1222.
29. Te Velde AA, van Kooyk Y, Braat H, Hommes DW, Dellemijn TA, Slors JF, *et al*. Increased expression of DC-SIGN+IL-12+IL-18+ and CD83+IL-12-IL-18- dendritic cell populations in the colonic mucosa of patients with Crohn's disease. *Eur J Immunol* 2003;**33:**143–151.
30. Duperrier K, Velten FW, Bohlender J, Demory A, Metharom P, Goerdt S. Immunosuppressive agents mediate reduced allostimulatory properties of myeloid-derived dendritic cells despite induction of divergent molecular phenotypes. *Mol Immunol* 2005;**42:**1531–1540.
31. Yu DT, Clements PJ, Paulus HE, Peter JB, Levy J, Barnett EV. Human lymphocyte subpopulations. Effect of corticosteroids. *J Clin Invest* 1974;**53:**565–571.
32. Wasowska BA, Zheng XX, Strom TB, Kupieck-Weglinski JW. Adjunctive rapamycin and CsA treatment inhibits monocyte/macrophage associated cytokines/chemokines in sensitized cardiac graft recipients. *Transplantation* 2001;**71:**1179–1183.
33. Sarwal M, Chua MS, Kambham N, Hsieh SC, Satterwhite T, Masek M, *et al*. Molecular heterogeneity in acute renal allograft rejection identified by DNA microarray profiling. *N Engl J Med* 2003;**349:**125–138.
34. Robson NC, Beacock-Sharp H, Donachie AM, Mowat AM. The role of antigen-presenting cells and interleukin-12 in the priming of antigen-specific CD4+ T cells by immune stimulating complexes. *Immunology* 2003;**110:**95–104.
35. Giomarelli P, Scolletta S, Borrelli E, Biagioli B. Myocardial and lung injury after cardiopulmonary bypass: role of interleukin (IL)-10. *Ann Thorac Surg* 2003;**76:**117–123.
36. Azzawi M, Hasleton PS, Grant SC, Stewart JP, Hutchinson IV. Interleukin-10 in human heart transplantation: an in situ hybridization study. The Manchester Transplant Cytokine Group. *J Heart Lung Transplant* 1995;**14:**519–528.
37. Di Carlo E, Coletti A, Modesti A, Giovarelli M, Forni G, Musiani P. Local release of interleukin-10 by transfected mouse adenocarcinoma cells exhibits pro- and anti-inflammatory activity and results in a delayed tumor rejection. *Eur Cytokine Netw* 1998;**9:**61–68.
38. Mocellin S, Panelli MC, Wang E, Nagorsen D, Marincola FM. The dual role of IL-10. *Trends Immunol* 2003;**24:**36–43.
39. Bielawska-Pohl A, Crola C, Caignard A, Gaudin C, Dus D, Kieda C, *et al*. Human NK cells lyse organ-specific endothelial cells: analysis of adhesion and cytotoxic mechanisms. *J Immunol* 2005;**174:**5573–5582.
40. Uehara S, Chase CM, Kitchens WH, Rose HS, Colvin RB, Russell PS, *et al*. NK cells can trigger allograft vasculopathy: the role of hybrid resistance in solid organ allografts. *J Immunol* 2005;**175:**3424–3430.
41. Petersson E, Qi Z, Ekberg H, Ostraat O, Dohlsten M, Hedlund G. Activation of alloreactive natural killer cells is resistant to cyclosporine. *Transplantation* 1997;**63:**1138–1144.